Computer Methods in Biomechanics and Biomedical Engineering,
2003 VOL. 6 (2), pp. 99–111

Taylor & Francis
healthsciences

A Model of Human Muscle Energy Expenditure

BRIAN R. UMBERGER*, KARIN G.M. GERRITSEN and PHILIP E. MARTIN

Exercise & Sport Research Institute, Arizona State University, Box 870404, Tempe, AZ 85287-0404, USA

(Received 7 January 2002; In final form 20 December 2002)

A model of muscle energy expenditure was developed for predicting thermal, as well as mechanical energy liberation during simulated muscle contractions. The model was designed to yield energy (heat and work) rate predictions appropriate for human skeletal muscle contracting at normal body temperature. The basic form of the present model is similar to many previous models of muscle energy expenditure, but parameter values were based almost entirely on mammalian muscle data, with preference given to human data where possible. Nonlinear phenomena associated with submaximal activation were also incorporated. The muscle energy model was evaluated at varying levels of complexity, ranging from simulated contractions of isolated muscle, to simulations of whole body locomotion. In all cases, acceptable agreement was found between simulated and experimental energy liberation. The present model should be useful in future studies of the energetics of human movement using forward dynamic computer simulation.

Keywords: Biomechanics; Computer simulation; Energetics; Musculoskeletal modeling

INTRODUCTION

Computer simulation of human movement using multiple-segment, multiple-muscle models has become commonplace over the last decade. Most models use some form of the standard two- or three-element Hill-type muscle model [1–3], which allow for a straightforward assessment of the mechanical energetics of the activity being studied. Unfortunately, thermal energy liberation cannot be effectively predicted using the standard Hill-type models. Hill [4] initially suggested that the constant "*a*" and "*b*" in his force-velocity equation bore a broader energetic significance, however, these relations have not turned out to be true in general [5,6]. Thus, Hill-type muscle models do not allow for a complete description of the energetics of muscle contraction. An estimate of the total energy (thermal plus mechanical) liberated during a simulated activity would be useful, as minimization of metabolic energy expenditure is believed to be an important criterion for human and animal locomotion [7]. To this end, many models of muscle energy liberation have been developed [8–21], most for use in conjunction with a mechanical muscle model.

The general form of a muscle energetics model can be derived from a straightforward application of thermodynamic principles to biological systems [22]. While a generic muscle energy model can be readily formulated, a major challenge is the determination of appropriate parameter values and scaling relations. Many of the models proposed to date rely heavily on data from amphibian muscle [8,9,12,13,17–20], which has a considerably greater energy rate than mammalian muscle even when expressed in normalized form [5,23]. These models also suffer from uncertainties regarding scaling of data collected at low temperatures to normal body temperature. Other models do not adequately account for heat production during muscle lengthening [8,10,14,15,17], despite the prevalence of eccentric muscle activity in human movement. Some alternative models avoid many of these problems [11,16], but are not formulated in a manner that can be incorporated into the multiple-muscle musculoskeletal models commonly used in computer simulations.

A common assumption used in models of muscle energy production [12,13,17–20] is that energy output at submaximal activation is simply a linearly scaled down version of energy output at full activation (i.e. constant economy of isometric force production is assumed). Other models predict that force production is relatively less costly at low activation than at high activation [8,15]. However,

*Corresponding author. Tel.: +1-480-965-7528. Fax: +1-480-965-8108. E-mail: brian.umberger@asu.edu

ISSN 1025-5842 print/ISSN 1476-8259 online
DOI: 10.1080/1025584031000091678

most of the available evidence suggests that energy rates at low muscle activation are actually higher than would be expected given a linear scaling with activation [21,24–29]. Another factor not accounted for by current models is that the so called "shortening heat" [4] that is present at full activation is markedly suppressed when shortening occurs during submaximal contractions [21,25–27]. Such activation-dependent phenomena should be incorporated into models of muscle energy expenditure, as most activities in which energy expenditure is considered important are performed submaximally. Additionally, very few models [8–10,15] have accounted for between-muscle fibre type differences, despite human fast twitch (FT) muscle fibres have an energy rate four to six times greater than human slow twitch (ST) fibers [23,24].

Perhaps the greatest criticism that can be lodged against existing models is that most have not been adequately evaluated to demonstrate that they yield reasonable predictions of human energy output for a variety of contractile conditions. Estimates of muscle heat production during isometric contractions in humans were first published in the 1940s [30], and have been commonly available for the last 25 years [24,28,29,31]. Surprisingly, very few investigators [15] have compared the output of their models with any of these data. Recently, precise measures of human muscle heat production have also been reported during dynamic contractions [32], which allows for a more complete evaluation of model performance.

The purpose of this study was to develop and evaluate a phenomenological model of skeletal muscle energy expenditure for use with a Hill-type muscle model. The major objective was that the model be appropriate for predicting human muscle energy expenditure over the full activation range, and for varying contractile conditions. The model was based almost entirely on mammalian muscle data, with preference given to human data where possible. We also tried to avoid scaling model output by assigning (or fitting) parameter values that could not be justified from basic experimental data. Predications from the model were evaluated by performing simulations at three levels of complexity; isolated muscle actions, single joint motion and whole body movement.

MODEL DERIVATION

Mechanical Muscle Model

In the present study, a modification of the Hill-type muscle model described by van Soest and Bobbert [1] was used. The model was modified to better account for: (1) force production at submaximal activation and (2) effects of between-muscle fibre type differences. The model consisted of a contractile element (CE) and a series elastic element (SEE). When modeling complete muscle-joint systems, parallel elastic effects were lumped at the joint level with other passive structures [2]. Only the current modifications to the model will be covered in detail. A full description of the basic model can be found in Ref. [33].

The right hand side of the force–velocity equation was originally scaled by van Soest and Bobbert [1] by a quantity FACTOR $= \min(1, 3.33 \cdot \mathrm{ACT})$ which makes maximal CE velocity ($V_{\mathrm{CE(MAX)}}$) depend on ACT when muscle active state is low. With this approach $V_{\mathrm{CE(MAX)}}$ is constant unless ACT is below 30% of maximum, which is not consistent with human muscle data [34,35]. To better represent the dependence of $V_{\mathrm{CE(MAX)}}$ on muscle activation, we scale A_{REL} by a quantity $A_{\mathrm{FACTOR}} = \mathrm{ACT}^{-0.3}$ which reduces $V_{\mathrm{CE(MAX)}}$ at submaximal activation in approximately the same manner as observed by Chow and Darling [34]. This latter approach to scaling A_{REL} is essentially the same as reported by Hatze and Buys [15] and requires a non-zero resting active state. At very low activation (e.g. ACT $= 0.05$), when primarily ST fibres would be recruited, $V_{\mathrm{CE(MAX)}}$ is reduced by a factor of about 2.5, which is consistent with the difference in $V_{\mathrm{CE(MAX)}}$ usually reported between ST and FT fibres in mammalian muscle [36–38]. The progressive increase in $V_{\mathrm{CE(MAX)}}$ with increasing activation caused by $\mathrm{A_{FACTOR}}$ is thought to be due to recruitment of faster motor units according to the size principle [34].

The normalized Hill constants A_{REL} ($= a/F_{\mathrm{MAX}}$) and B_{REL} ($= b/L_{\mathrm{CE(OPT)}}$) determine the shape of the force–velocity curve and maximal shortening velocity, and consequently affect the power that can be generated for a given maximal isometric force (F_{MAX}). The Hill constants also determine the shortening speed at which power output is maximal. When many muscles are to be modelled simultaneously, the common approach has been to assign all muscles the same normalized Hill constants [1,3]. This assumes that all muscles have the same $V_{\mathrm{CE(MAX)}}$ and same shaped force–velocity curve, regardless of fibre type composition. A similar $V_{\mathrm{CE(MAX)}}$ in all modelled muscle seems appropriate, based on the knowledge that nearly all human muscles are of mixed fibre type [39], and a muscle will exert tension until it reaches $V_{\mathrm{CE(MAX)}}$ of its fastest fibres [3,40] On the other hand, assuming that all muscles have the same shaped force–velocity curve is not as reasonable. Given the much lower power capability of ST fibres, one would expect a muscle with more ST fibres to have a force–velocity relation with more curvature than a muscle with more FT fibres. Winters and Stark [41] have described a simple means for determining A_{REL}, based on whole muscle fibre type composition

$$A_{\mathrm{REL}} = 0.1 + 0.4(\%\mathrm{FT}/100) \tag{1}$$

where %FT is the percentage of FT fibres (Type IIa and IIb). Application of Eq. (1) allows for a more appropriate representation of differences in the power capabilities of muscles with varying fibre type compositions, both within (m. soleus vs. m. rectus femoris) and between

individuals (endurance athlete vs. power athlete). The B_{REL} constant is then determined from the relation

$$B_{REL} = A_{REL}\tilde{V}_{CE(MAX)} \quad (2)$$

where $\tilde{V}_{CE} = V_{CE}/L_{CE(OPT)}$ is expressed in $L_{CE(OPT)}s^{-1}$. A value of 12 $L_{CE(OPT)}s^{-1}$ is used for $\tilde{V}_{CE(MAX)}$ in the present study, which is comparable to values used in similar muscle models (10–13 $L_{CE(OPT)}\,s^{-1}$; 1,3,41) and is consistent with recent *in vivo* estimates of $\tilde{V}_{CE(MAX)}$ in human muscle [42].

Delays between the input of an idealized neurocontrol signal (STIM) and the development of muscle active state (ACT) were modelled as a first-order process [43]. The two rate constants (c_1 and c_2) in the differential equation describing activation dynamics are related to the activation and deactivation time constants by

$$c_1 = \frac{1}{\tau_{ACT}} - c_2 \text{ and } c_2 = \frac{1}{\tau_{DEACT}}. \quad (3)$$

Time constants for activation and deactivation have also commonly been assumed to be the same for all muscles in large dimensional models, but can be personalized by scaling with muscle fibre type distribution. Our formulation for determining time constants based on fibre type distribution is founded in the knowledge that there is a similar ratio of the time course of activation dynamics to $V_{CE(MAX)}$ across mammalian muscles of different fibre types [3,44]. Assuming again that the $V_{CE(MAX)}$ ratio for FT to ST fibres is 2.5:1, we use the following empirical relation to determine time constants for activation (τ_{ACT}) and deactivation (τ_{DEACT}):

$$\tau = A_1 - A_2 \times \%FT, \quad (4)$$

where $A_1 = 80$ ms and $A_2 = 0.47$ ms for τ_{ACT} and $A_1 = 90$ ms and $A_2 = 0.56$ ms for τ_{DEACT}. This approach is also similar to Winters and Stark [41], but is independent of muscle mass. For muscles of mixed fibre type this approach gives time constants consistent with those used in other studies [45, 46], and also gives active state and muscle force rise and fall times similar to, but slightly faster than reported by van Zandwijk and colleagues [47].

In order to relate mechanical and thermal energy estimates, muscle masses must be known. Muscle mass is related to F_{MAX} through the physiological cross sectional area (PCSA). F_{MAX} is calculated as

$$F_{MAX} = \sigma PCSA \quad (5)$$

where σ is specific tension (in Pa) and PCSA is in m^2. Muscle mass (kg) is related to PCSA by

$$\text{mass} = PCSA\,\rho L_{CE(OPT)} \quad (6)$$

where ρ is muscle density (1059.7 kg m^{-3} for mammalian muscle; [48]) and $L_{CE(OPT)}$ is in m. Widely ranging values of σ (0.10–1.00 MPa) for human muscle have been reported in the literature [49,50]. However, several recent *in vivo [51,52]* and *in vitro* [23,38,53] estimates of σ for human muscle have been reported between 0.15 and 0.30 MPa, which is consistent with the wealth of data on other mammalian muscles [36,37,54]. Muscle masses in the present model were based on a value of $\sigma = 0.25$ MPa.

Muscle Energy Expenditure Model

Following the traditional approach of partitioning muscle energy liberation [5,6,15,19], the total rate of muscle energy expenditure ($\dot{E}$), expressed in Watts per kilogram of muscle tissue (W kg^{-1}), was represented as the sum of four terms

$$\dot{E} = \dot{h}_A + \dot{h}_M + \dot{h}_{SL} + \dot{w}_{CE}. \quad (7)$$

The four terms on the right hand side of Eq. (7) are the activation heat rate ($\dot{h}_A$), the maintenance heat rate ($\dot{h}_M$), the shortening/lengthening heat rate ($\dot{h}_{SL}$) and the mechanical work rate of the CE ($\dot{w}_{CE}$). The separation of $\dot{h}_M$ and $\dot{h}_{SL}$ into two terms is only a matter of convenience as both are thought to be due primarily to actomyosin interaction, while heat due to activation of muscle ($\dot{h}_A$) is believed to be associated primarily with sarcoplasmic reticular ion transport [5,6]. Expressions for the terms on the right hand side of Eq. (7) are first derived for the case of full activation, and then appropriate scaling factors are developed to account for submaximal activation.

Activation and Maintenance Heat Rate

Although they likely derive from different sources, $\dot{h}_A$ and $\dot{h}_M$ can conveniently be considered together [15]. Bolstad and Ersland [24] studied heat production in human muscles of various fibre types *in vivo*, and developed an expression for the combined ($\dot{h}_A + \dot{h}_M$) at full activation as a function of muscle fibre type. For simplicity, $\dot{h}_{AM}$ will subsequently be used to represent the combined term ($\dot{h}_A + \dot{h}_M$). The expression for $\dot{h}_{AM}$ is linearly related to %FT fibres ($r^2 = 0.81$) and has the form

$$\dot{h}_{AM} = 1.28 \times \%FT + 25. \quad (8)$$

Thus, theoretical human muscles with 100% FT and 100% ST fibres would have heat rates of 153 and 25 W kg^{-1}, respectively, at maximal isometric activation. This is similar to the FT–ST heat rate ratio observed in other mammals [5].

Experimentally, $\dot{h}_A$ is usually distinguished from $\dot{h}_M$ by stretching muscle fibres to such a length that actomyosin interaction is prevented. The heat production remaining at such lengths is considered to represent that portion associated with activating the muscle. The proportion of $\dot{h}_{AM}$ remaining when actomyosin interaction is prevented varies across species, but is about 40% in mammalian muscle [5,6]. Thus, 40% of $\dot{h}_{AM}$ is assigned to the activation heat rate and 60% represents the maintenance

heat rate. Recent *in vitro* estimates of ATP utilization in skinned human muscle fibres [23,55] are generally consistent with our partitioning of $\dot{h}_{AM}$. However, these recent results also suggest that the intercept in Eq. (8) may be slightly underestimated, while the slope in Eq. (8) may be overestimated. Fortunately, if the intercept and slope in Eq. (8) are slightly in error, there would still be little effect on the predicted $\dot{h}_{AM}$ for a muscle of mixed fibre type.

Shortening and Lengthening Heat Rate

During CE shortening, the rate of heat production above $\dot{h}_{AM}$ has classically been modelled as the product of a coefficient (α_S) and V_{CE} [4]. Hill [56] has shown for frog muscle that the coefficient α_S actually depends on F_{CE} rather than being a linear function of V_{CE}. However, shortening heat rates from other species [6], including mammals [36,57], often do show a nearly linear dependence on V_{CE}. Similar results are found for shortening ATP rates in mammalian muscle [58,59]. Our formulation of $\dot{h}_{SL}$ during muscle shortening is based on the findings by Barclay *et al.* [36] that the total heat rate for ST fibres shortening at their maximal velocity ($V_{CE(MAX\text{-}ST)}$) is approximately 5 times greater than $\dot{h}_{AM}$ for ST fibres. However, the total heat rate for FT fibres shortening at their maximal velocity ($V_{CE(MAX\text{-}FT)}$) is only 1.5–3 times greater than $\dot{h}_{AM}$ for FT fibres [36,57]. The shortening heat coefficients for ST and FT fibres are thus calculated as

$$\alpha_{S(ST)} = \frac{4 \times 25}{\tilde{V}_{CE(MAX-ST)}} \tag{9}$$

and

$$\alpha_{S(FT)} = \frac{1 \times 153}{\tilde{V}_{CE(MAX-FT)}} \tag{10}$$

where $\tilde{V}_{CE(MAX-FT)}$ is defined by the Hill coefficients A_{REL} and B_{REL}, and is assumed to be 2.5 times greater than $\tilde{V}_{CE(MAX-ST)}$. The shortening heat rate is then given by

$$\dot{h}_{SL} = -\alpha_{S(ST)}\tilde{V}_{CE}(1 - \%FT/100) - \alpha_{S(FT)}\tilde{V}_{CE}(\%FT/100), \tag{11}$$

for values of $\tilde{V}_{CE} \leq 0$. Little is known about the energetic fate of ST muscle fibres when the whole muscle shortens at greater than $V_{CE(MAX\text{-}ST)}$. In the present model, we assume that the first term on the right hand side of Eq. (11) cannot exceed $100\,W \cdot kg^{-1}$ (i.e. $\alpha_{S(ST)} \cdot V_{CE(MAX-ST)}$). This is equivalent to assuming that ST fibres continue to liberate energy at their maximal rate if the whole muscle is shortening faster than the maximal velocity of ST fibres. From a practical standpoint, CE velocity is unlikely to exceed $V_{CE(MAX\text{-}ST)}$ during simulations of submaximal activities (e.g. walking, pedalling, etc.), except possibly for very brief periods.

Much less is known about heat production in lengthening muscle, making it harder to develop a physiologically sound expression for the lengthening heat rate. The limited data suggest that the rate of extra heat production in lengthening can also be represented as the product of a coefficient (α_L) and CE velocity, with a slope somewhat greater than in shortening [6]. Surprisingly good agreement (see "Results" section) with experimental data [16,60] can be obtained by defining a lengthening heat coefficient that is a simple multiple of α_S. The value used for the lengthening heat coefficient,

$$\alpha_L = 4\,\alpha_{S(ST)} \tag{12}$$

not only yields results that are consistent with isolated muscle data at maximal activation, but also results in a similar sensitivity of total energy rate to load and velocity in submaximal cyclic contractions as was found experimentally in humans by Hawkins and Molé [16]. The lengthening heat rate is then given by

$$\dot{h}_{SL} = \alpha_L\,\tilde{V}_{CE} \tag{13}$$

when $\tilde{V}_{CE} > 0$. Some isolated muscle data suggest that α_L may be negative for very slow lengthening velocities [6]. However, ATP turnover has actually been reported to increase slightly during slow ($6^\circ\,s^{-1}$) eccentric work in human dorsiflexors, compared with the isometric case for the same force production [61]. Given that muscle activation was probably also lower during the eccentric work, a positive α_L at all lengthening velocities seems appropriate.

Mechanical Work Rate

The mass specific mechanical work rate is given by

$$\dot{w}_{CE} = -\frac{F_{CE}\,V_{CE}}{m}, \tag{14}$$

where m is the mass of the muscle being considered. In general, $\dot{w}_{CE}$ is not equal to the mechanical work rate of the entire musculotendon unit ($\dot{w}_{MT}$), which includes any work done by (or on) the SEE. The distinction between $\dot{w}_{CE}$ and $\dot{w}_{MT}$ becomes important when considering efficiency of the CE vs. efficiency of the entire musculotendon unit.

Scaling Factors

Scaling factors are needed to account for the length and activation dependence of $\dot{h}_{AM}$ and $\dot{h}_{SL}$, and the dependence

of total heat rate on the metabolic working conditions (aerobic vs. anaerobic). Both $\dot{h}_M$ (60% of $\dot{h}_{AM}$) and $\dot{h}_{SL}$ are near maximal at $L_{CE(OPT)}$, and decrease approximately with the theoretical $F-L$ curve at lengths beyond $L_{CE(OPT)}$ [6,62,63]. However, there is little change in either $\dot{h}_M$ or $\dot{h}_{SL}$ at lengths shorter than $L_{CE(OPT)}$. To account for the length dependence of $\dot{h}_M$ and $\dot{h}_{SL}$ both quantities are scaled by the normalized, isometric force–length relation (F_{ISO}) when $L_{CE} > L_{CE(OPT)}$.

The major features of submaximal energy expenditure that are incorporated into the model are that $\dot{h}_{AM}$ is increased and $\dot{h}_{SL}$ is reduced (for shortening velocities) compared with a linear scaling of heat production with activation. The increase in $\dot{h}_{AM}$ at low activation is thought to be due at least in part to increased energy turnover associated with force and length oscillations in individual motor units operating at sub-fusion firing frequencies [21,28,29]. Force and length oscillations in individual motor units can occur even if whole muscle force and length are constant, due to the asynchronous nature of motor unit recruitment. The reason for a decrease in $\dot{h}_{SL}$ at low activation levels is less clear, but may also be due in part to force and length oscillations at low activation allowing length changes during shortening to be partly taken up by the SEE [21]. Other possible mechanisms for a decrease in $\dot{h}_{SL}$ based on cross-bridge kinetics have also been suggested [26,64].

To achieve the appropriate activation dependence, a scaling factor (A) that depends on STIM and ACT is first defined such that

$$A = \begin{cases} \text{STIM} & \text{when STIM} > \text{ACT} \\ (\text{STIM} + \text{ACT})/2 & \text{when STIM} \le \text{ACT}, \end{cases} \quad (15)$$

which accounts for the rapid rise and slow decay of heat production at the beginning and end of excitation, respectively. Equation (15) is similar to Schutte *et al.* [20], but incorporates the finding that heat production seems to fall faster than muscle active state [6]. Factors for scaling $\dot{h}_{AM}$ and $\dot{h}_{SL}$ that depend on A are then defined such that

$$A_{AM} = A^{0.6}, \quad (16)$$

and

$$A_S = A^{2.0}. \quad (17)$$

A nonlinear scaling of $\dot{h}_{SL}$ for lengthening velocities seems likely as well, but at present there are no supporting data. Therefore, $\dot{h}_{SL}$ is scaled by A_S when $\tilde{V}_{CE} \le 0$ and is scaled by A when $\tilde{V}_{CE} > 0$. The exponent in Eq. (16) provides an approximate fit to *in vivo* human muscle data presented by Saugen and Vøllestad [28], while the exponent in Eq. (17) results in substantial suppression of $\dot{h}_{SL}$ at low activation levels, consistent with the limited data available from Buschman *et al.* [25–27] and simulation results of Woledge. [21] In some cases, $\dot{h}_{SL}$ has actually been found to be negative [26]. However, based partly on the work by Woledge [21], we suspect that the reduction in shortening heat rate should not be as great in whole muscle as in isolated fibres.

The data on which the model is based were obtained under primarily anaerobic conditions. The intended applications, on the other hand, will mainly be simulation of submaximal, steady-state activities, representing aerobic working conditions. The total heat rate ($\dot{h}_A + \dot{h}_M + \dot{h}_{SL}$), therefore, needs to be scaled up to account for the greater heat liberation per mole ATP when resynthesis occurs via aerobic vs. anaerobic pathways [65–67]. Theoretically, the molar enthalpy change would be greater by a factor of two when ATP is resynthesized via oxidative pathways (72 kJ mol ATP^{-1}) rather than by a net breakdown of phosphocreatine (35 kJ mol ATP^{-1}). Given that the circulation-occluded contractions on which the current model parameters are based [24] surely involved a mix of phosphocreative and glycolytic (65 kJ mol ATP^{-1}) energy production, and no submaximal activity is "purely" aerobic, a factor lower than two seems appropriate. Based on the *in vivo* human muscle data reported by Gonzàlez-Alonso *et al.* [32], we define a scaling factor S, where $S = 1.0$ for primarily anaerobic conditions and $S = 1.5$ for primarily aerobic conditions.

Total Energy Rate

The total rate of energy liberation for a muscle in $W\,kg^{-1}$ total muscle mass is obtained from the following equation:

$$\text{if } L_{CE} \le L_{CE(OPT)},$$

$$\dot{E} = \dot{h}_{AM}\, A_{AM}\, S + \begin{cases} \left[-\alpha_{S(ST)}\, \tilde{V}_{CE}\,(1 - \%FT/100) - \alpha_{S(FT)}\, \tilde{V}_{CE}\,(\%FT/100)\right] A_s\, S & \text{if } \tilde{V}_{CE} \le 0 \\ \alpha_L\, \tilde{V}_{CE}\, A\, S & \text{if } \tilde{V}_{CE} > 0 \end{cases} - (F_{CE}\, V_{CE})/m \quad (18)$$

$$\text{if } L_{CE} > L_{CE(OPT),}$$

$$\dot{E} = (0.4 \times \dot{h}_{AM} + 0.6 \times \dot{h}_{AM} F_{ISO}) A_{AM} S + \begin{cases} \left[-\alpha_{S(ST)} \tilde{V}_{CE} (1 - \%FT/100) - \alpha_{S(FT)} \tilde{V}_{CE} (\%FT/100)\right] F_{ISO} A_s S & \text{if } \tilde{V}_{CE} \leq 0 \\ \alpha_L \tilde{V}_{CE} F_{ISO} A S & \text{if } \tilde{V}_{CE} > 0 \end{cases} - (F_{CE} V_{CE})/m$$

where the term $(-\alpha_{S(ST)}\tilde{V}_{CE}(1 - \%FT/100))$ can not exceed $(\alpha_{S(ST)} V_{CE(MAX\text{-}ST)})$. Finally, the total heat rate is not allowed to fall below $1.0\,W\,kg^{-1}$ when muscle active state is very low. This last condition approximates the resting energy rate for human skeletal muscle *in vivo* [68].

MODEL EVALUATION

The muscle energetics model was evaluated by generating computer simulations of isolated muscle contractions, single joint actions, and bipedal walking. The musculoskeletal model of Gerritsen *et al.* [45] was used in all simulations, with modifications made to the muscle model as described in the previous sections. Relevant parameter values for the muscles are given in Table I. Optimisations of muscle excitation patterns for the isolated muscle and single joint models were performed using a nonlinear simplex algorithm (MATLAB Optimization Toolbox, The MathWorks Inc., Natick, MA). Optimization for the walking model was performed using a modified version [69] of the global optimisation algorithm by Bremermann [70]. Model state equations were integrated using an Adams-type, predictor–corrector method with variable order and step size [71], and quadrature was performed using a spline-based routine [72].

TABLE I Parameter values for the muscle model that depend on muscle fibre type distribution

Muscle	%FT	A_{REL}	B_{REL}	τ_{ACT}	τ_{DEACT}
Soleus	20	0.18	2.16	70	83
Gastrocnemius	50	0.30	3.60	55	65
Vasti	50	0.30	3.60	55	65
Rectus femoris	65	0.36	4.32	48	56
Glutei	45	0.28	3.36	58	68
Hamstrings	35	0.24	2.88	63	74
Iliopsoas	50	0.30	3.60	55	65
Tibialis anterior	25	0.20	2.40	68	80

%FT is percentage of fast twitch muscle fibres, A_{REL} and B_{REL} are normalized Hill constants, and τ_{ACT} and τ_{DEACT} are activation and deactivation time constants in ms. Fibre type composition was based on Johnson *et al.* [39] and all other values were derived from fibre type using procedures described in the text. Other parameter values can be found in Gerritsen *et al.* [45].

Isolated Muscle Actions

Computer simulations were generated for isovelocity shortening and lengthening of all muscles from the plateau of a maximal isometric tetanus. The simulations were designed to be similar to protocols used to test isolated muscles [36]. The effects of the SEE were removed so that CE velocity would be equivalent to the externally imposed velocity. Simulations were also generated of isolated muscles undergoing cyclic contractions. Muscle excitation (STIM) onset and offset were optimised to produce maximal average power output over the course of a full shorten-lengthen cycle, as in the experiments performed by Barclay [54]. STIM amplitude was set to 1.0 during excitation and 0.0 during relaxation. SEE effects were included for the cyclic contractions.

Single Joint Motion

Planar, forward dynamic computer simulations of the seated knee extension/flexion task employed by González-Alonso *et al.* [32] were used to evaluate the model at the level of a single joint system. The knee joint centre is fixed relative to the crank arm axis in this experimental set up [73], thus the motion can be simulated as a four bar linkage. The right leg of the musculoskeletal model was oriented with the thigh segment horizontal and fixed in space. The shank segment was free to rotate at the knee joint, and the ankle joint was locked. Segments representing the ergometre crank arm and connecting rod completed the four bar linkage. Frictional and inertial loads consistent with a standard bicycle ergometre flywheel [74] were applied to the crank arm segment.

Muscle excitation patterns (onset, offset and amplitude) to mm. vasti and m. rectus femoris were optimised to produce cyclic knee extension and flexion over the range of joint angles from 80 (flexed) to 170° (extended) at an average power output of $30.7\,W\,kg^{-1}$ quadriceps muscle mass and a rate of 1 Hz [32]. Three complete cycles of motion were simulated, with the third cycle being subjected to analysis. The objective function was formulated to generate this movement pattern with minimal negative muscle work. The basis for the negative muscle work criterion was that the experimental protocol

[32,73] involved training subjects to perform the movement by contracting the quadriceps during the extension phase, relaxing the quadriceps on the flexion phase, and minimizing recruitment of the hamstrings at all times. The model was run using the optimised excitation patterns with $S = 1.0$ and again with $S = 1.5$ to simulate primarily anaerobic and aerobic metabolic conditions, respectively.

Locomotion

Planar, forward dynamic computer simulations of human walking were generated to evaluate the muscle energy model in a whole body activity. Walking is an especially relevant activity to use, as minimization of energy expenditure has long been associated with self-selected walking patterns [7]. One full step of walking was simulated, with muscle excitation patterns optimised using a criterion similar in form to Anderson and Pandy [9]. Muscle excitation patterns for each muscle were represented by three consecutive blocks, described by switching times and amplitudes (7 parameters per muscle). Muscle excitation parameters were sought that minimized differences between the final and initial states of the skeleton (segment angles and angular velocities), taking into account side-to-side differences, while simultaneously minimizing the energy expended per unit distance travelled. Initial segment velocities were included as optimisation parameters to allow the final motion to be consistent with the optimised muscle excitation patterns. To account for whole body metabolism, the proportion of total body mass not represented by the modelled muscles was assigned an energy rate of $1.2\,\mathrm{W\,kg^{-1}}$, which is the normal energy rate for standing [75]. Aerobic conditions ($S = 1.5$) were assumed for all walking simulations.

RESULTS

Isolated Muscle Actions

Result for the isolated muscle simulations are presented in Figs. 1–4, along with corresponding data from the literature. In most cases the results are shown for m. soleus (20% FT fibres) and m. rectus femoris (65% FT fibres), as these two muscles represented the extremes of fibre type distribution in the model. The dependence of force, power, total energy rate and mechanical efficiency on shortening velocity for m. soleus and m. rectus femoris during isovelocity ramps are shown in Fig. 1, with data from Barclay *et al.* [36] provided for comparison. The general pattern for each of these variables was very similar in all muscles, but a number of differences can be seen that depended on the fibre type composition of the muscle. The dependence of work, heat, and total energy output on lengthening velocity are likewise shown for m. soleus and m. rectus femoris in Fig. 2, in conjunction with results from Constable *et al.* [60] The work shown in Fig. 2 is work done on the CE, and is roughly twice the heat produced by the muscles at all lengthening speeds above $0.2\,V_{MAX}$. The accumulated work, heat and total energy in a series of three cyclic contractions for m. soleus and m. rectus femoris are shown in Fig. 3, contrasted with similar data from Barclay [54]. Work production was comparable to heat production for m. soleus, but was lower for m. rectus femoris. The dependence of total energy rate on force production in cyclic shortening and lengthening contractions at the same cycle rate is shown in Fig. 4 for mm. vasti. Note that for the same force production, muscle active state was lower for cyclic lengthening contractions than shortening contractions. Comparable *in vivo* estimates for humans made by Hawkins and Molé [16] are shown for comparison. Energy rate was approximately four times more sensitive to force production in concentric cyclic contractions than in eccentric cyclic contractions. Unlike the case for large-amplitude isovelocity lengthening at full activation, the net energy output was always positive for submaximal eccentric cyclic contractions.

Single Joint Motion

The knee extension/flexion simulations reproduced the motion pattern reported for the subjects in González-Alonso *et al.* [32]. Work was performed at almost the same average rate ($30.6\,\mathrm{W\,kg^{-1}}$), with very little negative muscle work ($<1\,\mathrm{W\,kg^{-1}}$), and at the same cycle rate (1 Hz) as the subjects. With the scaling factor S set to 1.0 (anaerobic conditions), the model quadriceps liberated energy at a rate of $61.5\,\mathrm{W\,kg^{-1}}$, compared with 57.9 to $67.4\,\mathrm{W\,kg^{-1}}$ over the course of the first 30 s epoch for the subjects. During this time interval anaerobic sources represented more than 70% of the total energy turnover in the subjects' quadriceps muscles [32]. With S equal to 1.5 (aerobic conditions), the quadriceps energy rate for the model was $77.0\,\mathrm{W\,kg^{-1}}$, compared with 78.1 to $81.8\,\mathrm{W\,kg^{-1}}$ over the time interval from 60 to 150 s for the subjects. In these later epochs anaerobic sources contributed less than 20% to total energy turnover in the subjects' quadriceps muscles.

Locomotion

The model walked one full step (right heel-strike to left heel-strike) at an average speed of $1.2\,\mathrm{m\,s^{-1}}$. Muscle active state profiles arising from the optimised muscle excitation patterns exhibited good agreement with experimental EMG data (Fig. 5A) and resulted in a smooth, normal looking walking pattern (Fig. 5B). The whole-body rate of energy expenditure (including non-involved tissues) was $4.4\,\mathrm{W\,kg^{-1}}$, compared with a typical range of values from 4.0 to $4.3\,\mathrm{W\,kg^{-1}}$ reported for humans walking at the same speed (reviewed in Ref. [75]).

DISCUSSION

The purpose of this study was to develop a model of muscle energy expenditure for use with a Hill-type muscle

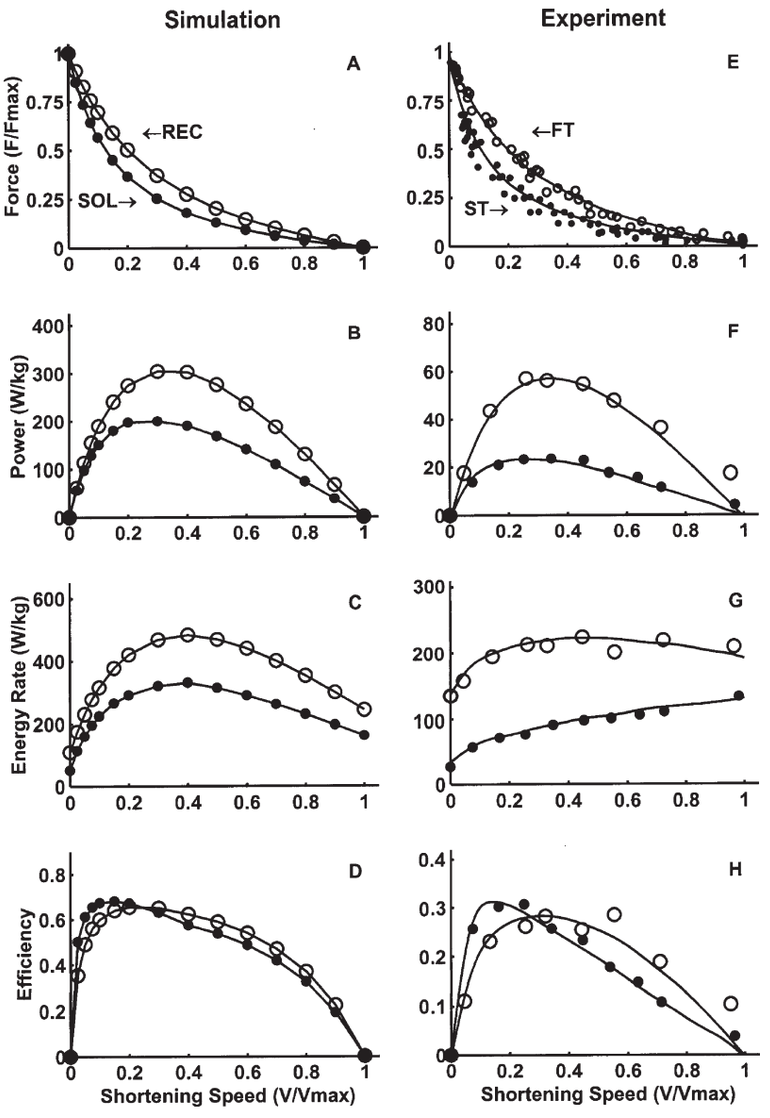

FIGURE 1 Dependence of force, power, energy rate and mechanical efficiency on CE shortening speed during simulated (A–D) and experimental (E–H) isovelocity concentric contractions. Experimental data are from Barclay *et al.* [36] for mouse ST and FT muscle fibre bundles. Closed and open circles represent soleus (20% FT fibres) and rectus femoris (65% FT fibres), respectively in panels A–D, and ST fibres and FT fibres, respectively in panels E–H.

model that would yield valid predictions of energy expenditure for human muscle at varying degrees of activation and under a wide variety of contractile conditions. To this end, model parameter values were based almost exclusively on mammalian data, giving preference to human data where available, and nonlinear phenomena related to submaximal activation were incorporated. Overall, the results showed reasonable predictions of energy expenditure when simulating human muscular activity at varying levels of complexity.

The dependence of force, power, energy rate and mechanical efficiency shown in Fig. 1 are similar to general trends in the results presented by Barclay *et al.* [36] for mouse skeletal muscle. In most cases, the differences between a primarily ST muscle (m. soleus) and a mostly FT muscle (m. rectus femoris) were consistent with, but intermediate to, differences found between purely ST and FT muscle fibres. Mass specific power output for m. rectus femoris was greater than for m. soleus, and peaked at a slightly higher shortening velocity. The mass specific total energy rate was substantially higher for m. rectus femoris than for m. soleus at intermediate shortening velocities, but this difference was greatly reduced at V_{MAX}. This is due to the shortening heat coefficient being much higher, in relative terms, for ST fibres than FT fibres [36]. The model also captured subtle difference in the shape of the experimental efficiency curves for ST and FT muscles. The efficiency curve for m. soleus had a sharper peak than m. rectus femoris, and this peak occurred at a slower shortening velocity. Peak efficiency in both muscles was

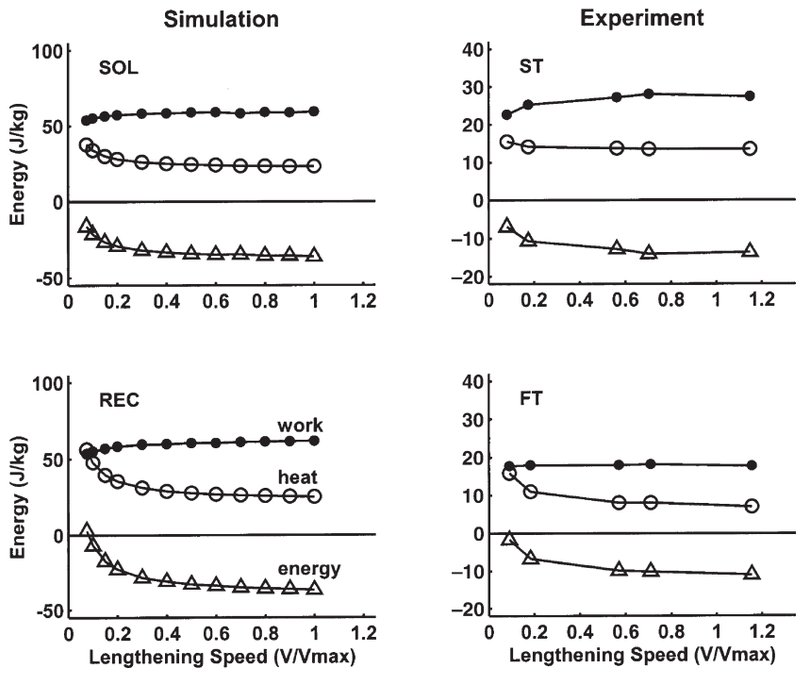

FIGURE 2 Dependence of work, heat and total energy on CE lengthening speed during simulated and experimental isovelocity stretches. Simulation data are shown for soleus (20% FT fibres) and rectus femoris (65% FT fibres), while experimental data are from Constable *et al.* [60] for mouse ST and FT muscle fibre bundles. The work shown is work done on the CE, and is about twice the heat produced at most lengthening speeds. Except at slow speeds, results are similar for both muscle fibre types.

about the same, which is also consistent with the experimental data. While our primary comparisons are with the work by Barclay and colleagues [36], model results are also generally consistent with data from other mammalian species obtained using very different experimental techniques [58,59].

Although the model results shown in Fig. 1 are qualitatively similar to data from other mammalian muscles, the power, energy rate and mechanical efficiency were all higher in the model. While there is no reason to believe that human and mouse skeletal muscle have the same mass specific energy rates (mechanical or thermal), much of

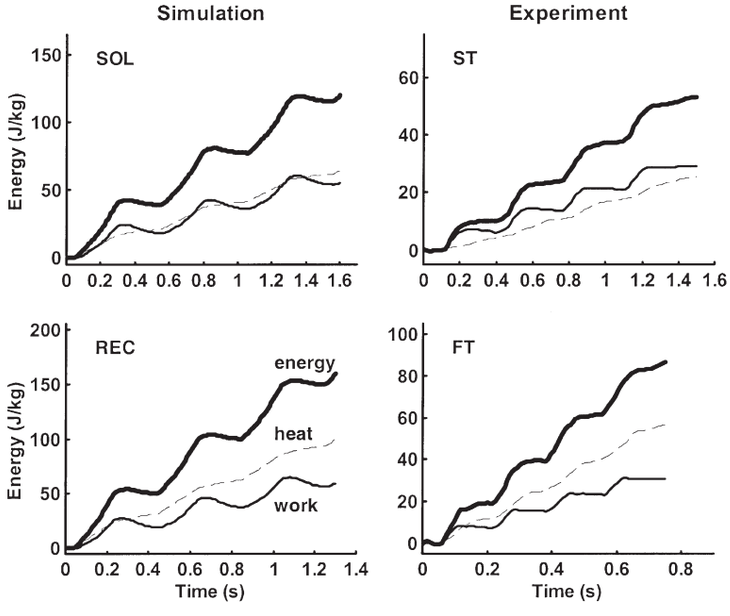

FIGURE 3 Work, heat and total energy liberation during simulated and experimental cyclic concentric contractions. Simulation data are shown for soleus (2 Hz) and rectus femoris (2.5 Hz), while experimental data are from Barclay [54] for mouse ST (3 Hz) and FT (6 Hz) muscle fibre bundles. Data are shown for each muscle at the cycle rate for which power output was greatest. Regardless of cycle rate, muscle excitation was timed to maximize net power over the full contraction–relaxation cycle at that speed.

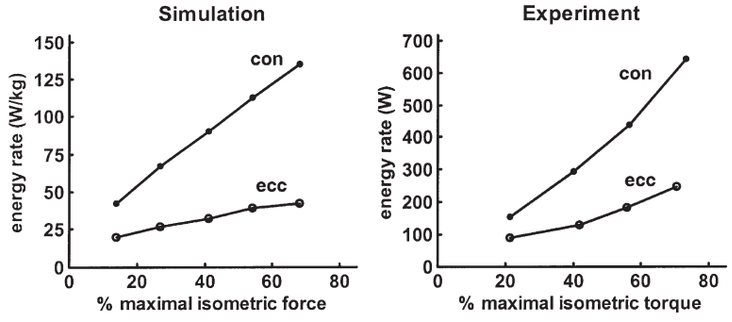

FIGURE 4 Dependence of total energy rate on intensity level during simulated and experimental concentric and eccentric cyclic contraction performed at the same rate. Simulation data are shown for the vasti group, while experimental data are from Hawkins and Molé [16], and were estimated from pulmonary oxygen consumption. The cycle rate for vasti was consistent with the cyclic knee extension/flexion rate used for the experimental data ($90° s^{-1}$). In both cases, total energy rate was approximately four times more sensitive to force production for concentric contractions than for eccentric contractions.

the difference can be explained by the fact that the data from Barclay *et al.* [36] were collected at 21°, while the model is based on data from human muscle at normal body temperature. There were also some differences between simulated and experimental data in the shapes of the curves. This may be because we were modelling whole muscles of mixed fibre type, while the experimental data came from homogeneous isolated fibre bundles. Differences in peak efficiencies between model and experimental data, which should be less temperature dependent, were quite large (over 0.60 for the model vs. 0.30 in the mouse muscles), and are worthy of further comment. Efficiencies shown in Fig. 1 represent "initial mechanical efficiencies" [36], and are defined as work/(heat + work) during the period of shortening only. Energy expended in recovery that occurs during or after contraction is not included. Thus, the model was set to the anaerobic mode for these simulations. If the same simulations are run in aerobic mode peak efficiencies are reduced to 0.50, and if a post contraction recovery heat [6] is included one obtains still lower efficiencies that are consistent with data from Hawkins and Molé [16].

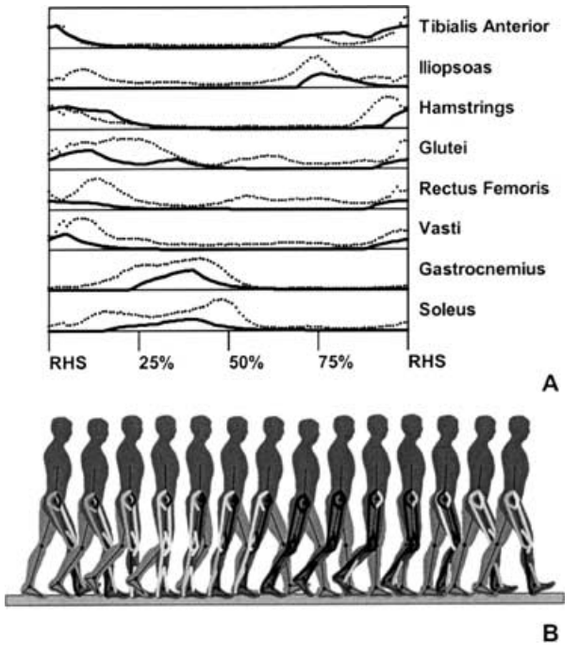

FIGURE 5 (A) Muscle active state profiles (solid lines) arising from the optimized muscle excitation patterns, and experimental EMG data (dotted lines) from a neurologically intact subject [45]. Overall, there was good agreement between the timing of muscle activation and the EMG bursts for most muscles. (B) Sequence of stick figures for one full stride of walking (right heel strike to right heel strike) using the optimized muscle excitation patterns. Lighter colored muscles denote periods of greater activation. A full stride was obtained by assuming bilateral symmetry.

A peak efficiency of 0.50 is considerably higher than the commonly cited value for humans of 0.25. However, there are many accounts in the literature of efficiency values ranging from 0.30 to 0.56 for human muscle [32,76,77]. Unfortunately, there are no studies of isovelocity or cyclic contraction in isolated human muscle fibres that reported both mechanical and thermal data to compare our results with. When human and rodent muscle fibres have been tested under the same conditions, human muscle is found to be 1.1–1.6 times more economical at generating force [23], and to have a more highly curved force–velocity relation [78]. While, higher economy does not necessarily imply higher efficiency, a causal relationship between greater curvature of the force–velocity relation and higher mechanical efficiency has been proposed [57,79]. Therefore, peak efficiencies in human muscle considerably higher than observed in rodent muscle seems at least plausible.

Energy liberation (thermal, mechanical and total) in simulated cyclic concentric contractions for m. soleus and m. rectus femoris (Fig. 3) also exhibited similarities with data from isolated mouse muscle fibers [54]. The general patterns in energy output were the same for both m. soleus and m. rectus femoris, with work production showing greater fluctuations over the contraction cycle than heat production. The major difference between the two muscles was that work production was comparable to heat production for m. soleus, but heat exceeded work for

m. rectus femoris. Analogous with results from Barclay [54], peak mechanical efficiency of m. soleus (0.50) was higher than for m. rectus femoris (0.37) in anaerobic cyclic concentric contractions. Mechanical efficiency in this case is calculated as the ratio of net work to total energy output, over the whole contraction/relaxation cycle. If the same cyclic contractions are performed under simulated aerobic conditions, peak efficiencies are reduced to approximately 0.38 and 0.27 for m. soleus and m. rectus femoris, respectively.

As with the case for muscle shortening, model results for isovelocity and cyclic eccentric contractions were qualitatively similar to corresponding experimental data. Patterns of heat, work and energy liberation for isovelocity lengthening were consistent with data presented by Constable *et al.* [60], and most importantly, captured the subtle difference between muscles of mostly ST and mostly FT fibre compositions (Fig. 2). Given that the work values shown in Fig. 2 are work done on the CE, and were greater than the heat produced at most lengthening velocities, the total energy output was negative for most speeds. This implies that some of the work done on the muscle during a stretch is stored, and interestingly, the SEE does not seem to be the major site of energy storage [60]. The present model does not attempt to represent the nature of this storage, but instead just accounts for the overall energetics of the muscle during stretch. Unlike the case where a large amount of work is done on the CE during an isovelocity stretch at full activation, total energy output during submaximal cyclic eccentric contractions was generally positive. The relative increases in total energy rate with increasing force production for concentric and eccentric cyclic contractions (Fig. 4) are similar to data from Hawkins and Molé [16], and are consistent with the notion that eccentric muscle work is more economical than concentric muscle work. Notably, the energetics of muscle lengthening for isovelocity and cyclic contractions were reproduced using the same simple lengthening heat rate coefficient.

Perhaps the best test of the current muscle energy model was the simulation of knee extension/flexion exercise, emulating the experiments conducted by González-Alonso *et al.* [32]. These investigators reported *in vivo* measures of heat and work in human skeletal muscle during dynamic contractions, and also provided estimates of the contributions made by the various energy pathways to the total enthalpy change. The agreement between model and subject energy rates was good for both anaerobic ($61.5\,W\,kg^{-1}$ compared with $57.9–67.4\,W\,kg^{-1}$, respectively) and aerobic ($77.0\,W\,kg^{-1}$ compared with $78.0–81.8\,W\,kg^{-1}$, respectively) metabolic conditions. The agreement between model and experimental data for aerobic condition is not surprising, as our selection of the aerobic scaling factor was based in large part on data from González-Alonso *et al.* [32]. However, the close agreement for aerobic conditions was only possible because of the concurrence between simulated and experimental energy rates for anaerobic condition. The good results for anaerobic conditions lend further confidence to the approach used in determining model parameter values. An even better fit to the González-Alonso *et al.* [32] data for aerobic condition could be obtained by using a value for S of 1.6, however, we do not feel that fitting the model exactly to the results of one experiment will necessarily improve the generality of the model.

Results from the walking optimisation also showed good agreement with experimental data. The timing of muscle activity bursts were generally consistent with experimental EMG data (Fig. 5A) and the patterns of motion were smooth and well coordinated (Fig. 5B). The whole body energy rate obtained for simulated walking ($4.4\,W\,kg^{-1}$) was also comparable to values observed in humans walking at the same speed [75]. The only other efforts of this kind in the literature [9,80] have reported energy rates that were considerably higher ($5.3–6.6\,W\,kg^{-1}$) than observed in humans walking at the speeds that were simulated. The primary differences between the muscle energy model in the present work and the models used in the studies by Anderson and Pandy [9] and Ogihara and Yamazaki [80] were the way the parameter values were assigned, and the approach used to scale energy rates for submaximal activation. These differences probably account for most of the discrepancies in the results.

The factor that we found the model to be most sensitive to was the assumption regarding muscle specific tension. While most recent reports of specific tension in human muscle fall between 0.15 and 0.30 MPa [23,38,51–53], musculoskeletal models have commonly used values between 0.40 and 1.50 MPa [41,81,82]. Specific tension affects the mass specific mechanical power output but not the thermal energy output, and thus affects mechanical efficiency. For example, using a specific tension of 0.50 MPa resulted in peak efficiency values of 0.85, compared with efficiency values of about 0.60 using our specific tension value of 0.25 MPa. If the model underestimates muscle heat production, this would partially offset a higher mass specific power output. However, we doubt that our model of heat production is off by enough to be consistent with specific tensions of 0.50 MPa, let alone values of 1.00–1.50 MPa.

CONCLUSION

A model of human muscle energy expenditure has been developed and evaluated at varying levels of complexity. The current model shares many similarities with previous efforts [15,20], but differs in the way parameter values and scaling factors were determined. Nearly all parameter values were based on mammalian data, with preference given to human data wherever possible. Overall, reasonable agreement was found between model predictions and experimental results at all three levels of complexity. Use of the present model of muscle energy expenditure in conjunction with forward dynamic

computer simulations should allow for a more complete understanding of the energetics of human movement.

Acknowledgements

We gratefully acknowledge Drs C.J. Barclay and D. Hawkins for allowing us to reproduce the experimental data from their studies that appeared in this article. The authors would also like to acknowledge the contributions made by Dr Akinori Nagano to this project. This work was supported in part by a National Science Foundation IGERT grant (DGE-9987619) titled "Musculoskeletal and Neural Adaptations in Form and Function".

References

[1] van Soest, A.J. and Bobbert, M.F. (1993) "The contribution of muscle properties in the control of explosive movements", *Biological Cybernetics* **69**, 195–204.

[2] Winters, J.M. (1990) "Hill-based muscle models: a systems engineering perspective", In: Winters, J.M. and Woo, S.L.Y., eds, Multiple Muscle Systems: Biomechanics and Movement Organization (Springer, New York), pp 69–91.

[3] Zajac, F.E. (1989) "Muscle and tendon: properties, models, scaling, and application to biomechanics and motor control", *Critical Reviews in Biomedical Engineering* **17**, 359–411.

[4] Hill, A.V. (1938) "The heat of shortening and the dynamic constants of muscle", *Proceedings of the Royal Society* **126B**, 136–195.

[5] Homsher, E. and Kean, C.J. (1978) "Skeletal muscle energetics and metabolism", *Annual Review of Physiology* **40**, 93–131.

[6] Woledge, R.C., Curtin, N.A. and Homsher, E. (1985) Energetic Aspects of Muscle Contraction (Academic Press, London).

[7] Ralston, H.J. (1976) "Energetics of human walking", In: Herman, R.M., Grillner, S., Stein, P.S.G. and Stuart, D.G., eds, Neural Control of Locomotion (Plenum Press, New York), pp 77–98.

[8] Anderson, F.C., "A dynamic optimization solution for a complete cycle of normal gait" Unpublished doctoral dissertation, The University of Texas (Austin).

[9] Anderson, F.C. and Pandy, M.G. (2001) "Dynamic optimization of human walking", *Journal of Biomechanical Engineering* **123**, 381–390.

[10] Davy, D.T. and Audu, M.L. (1987) "A dynamic optimization technique for predicting muscle forces in the swing phase of gait", *Journal of Biomechanics* **20**, 187–201.

[11] De Looze, M.P., Toussaint, H.M., Commissaris, D.A.C.M., Jans, M.P. and Sargeant, A.J. (1994) "Relationships between energy expenditure and positive and negative mechanical work in repetitive lifting and lowering", *Journal of Applied Physiology* **77**, 420–426.

[12] FitzHugh, R. (1977) "A model of optimal voluntary muscular control", *Journal of Mathematical Biology* **4**, 203–236.

[13] Hardt, D.E. (1978) "Determining muscle forces in the leg during normal human walking—an application and evaluation of optimization methods", *Journal of Biomechanical Engineering* **100**, 72–78.

[14] Hase, K. and Yamazaki, N. (1997) "Development of three-dimensional whole-body musculoskeletal model for various model analyses", *Japanese Society of Mechanical Engineers International Journal* **C40**, 25–32.

[15] Hatze, H. and Buys, J.D. (1997) "Energy-optimal controls in the mammalian neuromuscular system", *Biological Cybernetics* **27**, 9–20.

[16] Hawkins, D. and Molé, P. (1997) "Modeling energy expenditure associated with isometric, concentric, and eccentric muscle action at the knee", *Annuals of Biomedical Engineering* **25**, 822–830.

[17] Khang, G. and Zajac, F.E. (1989) "Paraplegic standing controlled by functional neuromuscular stimulation: part I—computer model and control-system design", *IEEE Transactions on Biomedical Engineering* **36**, 873–884.

[18] Minetti, A.E. and Alexander, R. McN. (1997) "A theory of metabolic costs for bipedal gaits", *Journal of Theoretical Biology* **186**, 467–476.

[19] Schutte, L.M., "Using musculoskeletal models to explore strategies for improving performance in electrical stimulation-induced leg cycle ergometry" Unpublished doctoral dissertation, Stanford University (Stanford).

[20] Schutte, L.M., Rodgers, M.M., Zajac, F.E. and Glaser, R.M. (1993) "Improving the efficacy of electrical stimulation-induced leg cycle ergometry: an analysis based on a dynamic musculoskeletal model", *IEEE Transactions on Rehabilitation Engineering* **1**, 109–125.

[21] Woledge, R.C. (1998) "Muscle energetics during unfused tetanic contractions: modeling the effects of series elasticity", In: Sugi, H. and Pollack, G. H., eds, Mechanisms of Work Production and Work Absorption in Muscle (Plenum Press, New York), pp 537–543.

[22] Wilkie, D.R. (1960) "Thermodynamics and the interpretation of biological heat measurements", *Progress in Biophysics and Biophysical Chemistry* **10**, 259–298.

[23] Stienen, G.J.M., Kiers, J.L., Bottinelli, R. and Reggiani, C. (1996) "Myofibrillar ATPase activity in skinned human skeletal muscle fibers: fiber type and temperature dependence", *Journal of Physiology* **493**, 299–307.

[24] Bolstad, G. and Ersland, A. (1978) "Energy metabolism, in different human skeletal muscles during voluntary isometric contraction", *European Journal of Applied Physiology* **38**, 171–179.

[25] Buschman, H.P.J., Elzinga, G. and Woledge, R.C. (1995) "Energetics of shortening depend on stimulation frequency in single muscle fibers from *Xenopus laevis* at 20°C", *European Journal of Physiology* **430**, 160–167.

[26] Buschman, H.P.J., Elzinga, G. and Woledge, R.C. (1996) "The effects of the level of activation and shortening velocity on energy output in type 3 muscle fibers from *Xenopus laevis*", *European Journal of Physiology* **433**, 153–159.

[27] Buschman, H.P.J., Linari, M., Elzinga, G. and Woledge, R.C. (1997) "Mechanical and energy characteristics during shortening in isolated type-1 muscle fibers from *Xenopus laevis* studied at maximal and submaximal activation", *European Journal of Physiology* **435**, 145–150.

[28] Saugen, E. and Vøllestad, N.K. (1995) "Nonlinear relationships between heat production and force during voluntary contractions in humans", *Journal of Applied Physiology* **79**, 2043–2049.

[29] Wiles, C.M. and Edwards, R.H.T. (1982) "Metabolic heat production in isometric ischaemic contractions of human adductor pollicis", *Clinical Physiology* **2**, 499–512.

[30] Barcroft, H. and Millen, J.L.E. (1947) "On the heat production in human muscle during voluntary contraction", *Journal of Physiology* **106**, 13P–14P.

[31] Edwards, R.H.T., Hill, D.K. and Jones, D.A. (1975) "Heat production and chemical changes during isometric contractions of the human quadriceps muscle", *Journal of Physiology* **251**, 303–315.

[32] González-Alonso, J., Quistorff, B., Krustrup, P., Bangsbo, J. and Saltin, B. (2000) "Heat production in human skeletal muscle at the onset of intense dynamic exercise", *Journal of Physiology* **524**, 603–615.

[33] Nagano, A. and Gerritsen, K.G.M. (2001) "Effects of neuromuscular strength training on vertical jumping performance–a computer simulation study", *Journal of Applied Biomechanics* **17**, 113–128.

[34] Chow, J.W. and Darling, W.G. (1999) "The maximum shortening velocity of muscle should be scaled with activation", *Journal of Applied Physiology* **86**, 1025–1031.

[35] Zahalak, G.I., Duffy, J., *et al.* (1976) "Partially activated human skeletal muscle: an experimental investigation of force, velocity, and EMG", *Journal of Applied Mechanics* **1**, 81–86.

[36] Barclay, C.J., Constable, J.K. and Gibbs, C.L. (1993) "Energetics of fast- and slow-twitch muscles of the mouse", *Journal of Physiology* **472**, 61–80.

[37] Close, R.I. (1972) "Dynamic properties of mammalian skeletal muscles", *Physiological Reviews* **52**, 129–197.

[38] Ruff, R.L. and Whittlesey, D. (1991) "Ca-, Sr-tension relationships and contraction velocities of human muscle fibers", *Muscle and Nerve* **14**, 1219–1226.

[39] Johnson, M.A., Polgar, J., Weightman, D. and Appleton, D. (1973) "Data on the distribution of fiber types in thirty-six human muscles:

an autopsy study", *Journal of the Neurological Sciences* **18**, 111–129.
[40] Claflin, D.R. and Faulkner, J.A. (1985) "Shortening velocity extrapolated to zero load and unloaded shortening velocity of whole rat skeletal muscle", *Journal of Physiology* **359**, 357–363.
[41] Winters, J.M. and Stark, L. (1988) "Estimated mechanical properties of synergistic muscles involved in movements of a variety of human joints", *Journal of Biomechanics* **21**, 1027–1041.
[42] De Ruiter, C.J., Didden, W.J.M., Jones, D.A. and De Haan, A. (2000) "The force–velocity relationship of human adductor pollicis muscle during stretch and the effects of fatigue", *Journal of Physiology* **526**, 671–681.
[43] He, J., Levine, W.S. and Loeb, G.E. (1991) "Feedback gains for correcting small perturbations to standing posture", *IEEE Transactions on Automatic Control* **36**, 322–332.
[44] Cheng, E.J., Brown, I.E. and Loeb, G.E. (2000) "Virtual muscle: a computational approach to understanding the effects of muscle properties on motor control", *Journal of Neuroscience Methods* **101**, 117–130.
[45] Gerritsen, K.G.M., van den Bogert, A.J., Hulliger, M. and Zernicker, R.F. (1998) "Intrinsic muscle properties facilitate locomotor control—a computer simulation study", *Motor Control* **2**, 206–220.
[46] Neptune, R.R. and Hull, M.L. (1998) "Evaluation of performance criteria for simulation of submaximal steady-state cycling using a forward dynamic model", *Journal of Biomechanical Engineering* **120**, 334–341.
[47] van Zandwijk, J.P., Bobbert, M.F., Harlaar, J. and Hof, A.L. (1998) "From twitch to tetanus for human muscle: experimental data and model predictions for m. triceps surae", *Biological Cybernetics* **79**, 121–130.
[48] Mendez, J. and Keys, A. (1960) "Density and composition of mammalian muscle", *Metabolism, Clinical and Experimental* **9**, 184–188.
[49] Haxton, H.A. (1944) "Absolute muscle force in the ankle flexors of man", *Journal of Applied Physiology* **103**, 267–273.
[50] Morris, C.B. (1948) "The measurement of the strength of muscle relative to the cross section", *Research Quarterly* **19**, 295–303.
[51] Chow, J.W., Darling, W.G. and Ehrhardt, J.C. (1999) "Determining the force–length–velocity relations of the quadriceps muscles: II. Maximum muscle stress", *Journal of Applied Biomechanics* **15**, 191–199.
[52] Maganaris, C.N., Baltzopoulos, V., Ball, D. and Sargeant, A.J. (2001) "*In vivo* specific tension of human skeletal muscle", *Journal of Applied Physiology* **90**, 865–872.
[53] Degens, H., Soop, M., Höök, P., Ljungqvist, O. and Larsson, L. (1999) "Post-operative effects on insulin resistance and specific tension of single human skeletal muscle fibers", *Clinical Science* **97**, 449–455.
[54] Barclay, C.J. (1994) "Efficiency of fast- and slow-twitch muscles of the mouse performing cyclic contractions", *Journal of Experimental Biology* **193**, 65–78.
[55] Szentesi, P., Zaremba, R., van Mechelen, W. and Stienen, G.J.M. (2001) "ATP utilization for calcium uptake and force production in different types of human skeletal muscle fibers", *Journal of Physiology* **531**, 393–403.
[56] Hill, A.V. (1964) "The effect of load on the heat of shortening of muscle", *Proceedings of the Royal Society* **159B**, 297–318.
[57] Barclay, C.J. (1996) "Mechanical efficiency and fatigue of fast and slow muscles of the mouse", *Journal of Physiology* **497**, 781–794.
[58] He, Z-H., Chillingworth, R.K., Brune, M., Corrie, J.E.T., Webb, M.R. and Ferenczi, M.A. (1999) "The efficiency of contraction in rabbit skeletal muscle fibers, determined from the rate of release of inorganic phosphate", *Journal of Physiology* **517**, 839–854.
[59] Sun, Y-B., Hilber, K. and Irving, M. (2001) "Effects of active shortening on the rate of ATP utilization by rabbit psoas muscle fibers", *Journal of Physiology* **531**, 781–791.
[60] Constable, J.K., Barclay, C.J. and Gibbs, C.L. (1997) "Energetics of lengthening in mouse and toad skeletal muscles", *Journal of Physiology* **505**, 205–215.
[61] Ryschon, T.W., Fowler, M.D., Wysong, R.E., Anthony, A.R. and Balaban, R.S. (1997) "Efficiency of human skeletal muscle *in vivo*: comparison of isometric, concentric, and eccentric muscle action", *Journal of Applied Physiology* **83**, 867–874.
[62] Hilber, K., Sun, Y-B. and Irving, M. (2001) "Effects of sarcomere length and temperature on the rate of ATP utilization by rabbit psoas muscle fibers", *Journal of Physiology* **531**, 771–780.
[63] Phillips, S.K. and Woledge, R.C. (1992) "A comparison of isometric force, maximum power and isometric heat rate as a function of sarcomere length in mouse skeletal muscle", *European Journal of Physiology* **420**, 578–583.
[64] Potma, E.J., Stienen, G.J.M., Barends, J.P.F. and Elzinga, G. (1994) "Myofibrillar ATPase activity and mechanical performance of skinned fibers from rabbit psoas muscle", *Journal of Physiology* **474**, 303–317.
[65] Curtin, N.A. and Woledge, R.C. (1978) "Energy changes and muscular concentration", *Physiological Reviews* **58**, 690–761.
[66] Wilkie, D.R. (1968) "Heat work and phosphorylcreatine breakdown in muscle", *Journal of Physiology* **195**, 157–183.
[67] Woledge, R.C. and Reilly, P.J. (1988) "Molar enthalpy change for hydrolysis of phosphorylcreatine under conditions in muscle cells", *Biophysics Journal* **54**, 97–104.
[68] Elia, M. (1992) "Organ and tissue contribution to metabolic rate", In: Kinney, J.M. and Tucker, H.N., eds, Energy Metabolism: Tissue Determinants and Cellular Corollaries (Raven Press, New York), pp 61–77.
[69] Winters, J.M., Nam, M.H. and Stark, L.W. (1984) "Modeling dynamical interactions between fast and slow movements: fast saccadic eye movement behavior in the presence of the slower VOR", *Mathematical Biosciences* **68**, 159–185.
[70] Bremermann, H. (1970) "A method of unconstrained global optimization", *Mathematical Biosciences* **9**, 1–15.
[71] Shampine, L.F. and Gordon, M.K. (1975) Computer Solution of Ordinary Differential Equations: The Initial Value Problem (Freeman, San Francisco).
[72] van Loan, C.F. (1997) Introduction to Scientific Computing (Prentice Hall, Upper Saddle River, NJ).
[73] Andersen, P., Adams, R.P., Sjøgaard, G., Thorboe, A. and Saltin, B. (1985) "Dynamic knee extension as model for study of isolated exercising muscle in human", *Journal of Applied Physiology* **59**, 1647–1653.
[74] Fregly, B.J., Zajac, F.E. and Dairaghi, C.A. (2000) "Bicycle drive system dynamics: theory and experimental validation", *Journal of Biomechanical Engineering* **122**, 446–452.
[75] Waters, R.L. and Mulroy, S. (1999) "The energy expenditure of normal and pathological gait", *Gait and Posture* **9**, 207–231.
[76] Ahlborg, G. and Jensen-Urstad, M. (1991) "Arm blood flow at rest and during arm exercise", *Journal of Applied Physiology* **70**, 928–933.
[77] Poole, D.C., Gaesser, G.A., Hogan, M.C., Knight, D.R. and Wagner, P.D. (1992) "Pulmonary and leg VO2 during submaximal exercise: implications for muscular efficiency", *Journal of Applied Physiology* **72**, 805–810.
[78] Bottinelli, R., Canepari, M., Pellegrino, M.A. and Reggiani, C. (1996) "Force–velocity properties of human skeletal muscle fibers: myosin heavy chain isoform and temperature dependence", *Journal of Physiology* **495**, 573–586.
[79] Woledge, R.C. (1968) "The energetics of tortoise muscle", *Journal of Physiology* **197**, 685–707.
[80] Ogihara, N. and Yamazaki, N. (2001) "Generation of human bipedal locomotion by a bio-mimetic neuro-musculo-skeletal model", *Biological Cybernetics* **84**, 1–11.
[81] Pedotti, A., Krishnan, V.V. and Stark, L. (1978) "Optimization of muscle-force sequencing in human locomotion", *Mathematical Biosciences* **38**, 57–76.
[82] Yoshihuku, Y. and Herzog, H. (1990) "Optimal design parameters of the bicycle-rider system for maximal muscle power output", *Journal of Biomechanics* **23**, 1069–1079.